Comparison of Nonlinear Filtering Algorithms in Ground Moving Target Indicator (GMTI) Tracking

Mahendra Mallick[a], T. Kirubarajan[b], Sanjeev Arulampalam[c]

mallick@alphatech.com, kiruba@ee.uconn.edu, sanjeev@signal.dera.gov.uk

[a]ALPHATECH, Inc., 50 Mall Road, Burlington, MA 01803, U.S.A.

[b]University of Connecticut, Storrs, CT 06269-2157, U.S.A.

[c]Pattern & Information Processing Group, Signal & Imagery Department, DERA, St Andrews Rd, Malvern, Worcs, WR14 3PS, UK.

Abstract – *The ground moving target indicator (GMTI) radar sensor plays an important role in situation awareness of the battlefield, surveillance, and precision tracking of ground targets. The extended Kalman filter (EKF) is usually used either alone or in the Interacting Multiple Model (IMM) framework to solve nonlinear filtering problems. Since the GMTI measurement model is nonlinear, the use of an EKF is not the best solution. The particle filter (PF) has been shown recently as a robust algorithm for a wide range of nonlinear estimation problems. The disadvantage of particle filters is the high computational load. In this paper, we compare the performance of the EKF and PF for the GMTI measurement problem using the nearly constant velocity (NCV) model in two dimensions. We analyze the differences in the performance of the EKF and PF using simulated data..*

Keywords: Nonlinear Filtering, Extended Kalman Filter, Particle Filter, Ground Moving Target Indicator (GMTI) Measurement

1 Introduction

Airborne surveillance of ground moving vehicles and helicopters using the Ground Moving Target Indicator (GMTI) radar sensor was proved extremely successful during the 1991 Gulf War [1]. Measurements from a GMTI radar are range, azimuth, and range-rate. The GMTI measurements are nonlinear functions of the target state, which includes the position and velocity. The objective of the GMTI tracking is to estimate the state of a target sequentially by processing GMTI measurements from one or more sensors. The state estimation problem is nonlinear due to the nonlinear GMTI measurement model. The Bayesian approach [2],[8]-[15] provides a rigorous framework for estimating the state of a target in general conditions. In the Bayesian approach, the conditional posterior density of the state given the measurements is computed recursively. However, closed form solutions cannot be obtained in all cases. If the dynamic and measurement models are linear and the probability distributions are Gaussian, then the Kalman filter (KF) represents an optimal estimator in the Bayesian framework. When the dynamic or measurement model is nonlinear or the distributions are non-Gaussian, numerical solutions using the Bayesian approach are required [8]-[15].

The extended Kalman filter (EKF) [2]-[6] and Interacting Multiple Model (IMM) filter [6],[7] are widely used as approximate filters for nonlinear filtering problems. In recent years, the particle filter (PF) [8]-[15] has proven to be a robust and numerically efficient approach for nonlinear filtering problems. Pioneering work using the PF for the tracking problem was performed by Gordon, Salmond, and Smith in [8]. Challa presents an excellent review of the applications of the PF to a wide range of tracking problems in [14]. In this paper, we compare the performances of the EKF and PF using the GMTI measurements.

The Cartesian coordinates for position and velocity are commonly used to represent the target state for most ground target tracking problems. A topographic coordinate frame (TCF) [3] with origin at a given point on the WGS 84 reference ellipsoid and axes along the local East, North, and upward directions is used for tracking ground targets. Motion of vehicles on the surface of the Earth is more complex than air targets due to the three-dimensional terrain and motion constraints impose by the terrain and road networks. In order to keep our analysis simple, we ignore the motion of the target on the 3D terrain and the effects of road networks. We assume that the target moves in the XY plane with a nearly constant velocity (NCV) motion and the radar sensor moves with constant velocity at a fixed height above the XY plane.

Sections 2 and 3 present the dynamic model and GMTI measurement models, respectively. In the EKF, linearization is usually performed about the predicted state. The measurement-updated state can be further improved by iteratively computing the updated state , measurement gradient matrix, gain , and measurement updated covariance matrix. EKF with this extension is known as the iterated EKF (IEKF) [5],[6]. In order to gain a clear understanding of the PF algorithm it is necessary to understand the general recursive Bayesian framework[8],[9],[12],[14]. We describe the algorithms for the IEKF, general recursive Bayesian estimation, and PF in Sections 4, 5, and 6, respectively. Sections 7 and 8 present numerical results and conclusions.

2 Kinematic Model

We consider the nearly constant velocity (NCV) motion of a target in the XY plane. Let $\mathbf{x}(t) \in \Re^n$ denote the state of the target at time t. The state consists of the position and velocity:

$$(2-1) \qquad \mathbf{x}(t) := \begin{bmatrix} x(t) & y(t) & \dot{x}(t) & \dot{y}(t) \end{bmatrix}'.$$

The continuous time dynamics of the state for the NCV motion is described by [5]

$$(2-2) \qquad \frac{d\mathbf{x}(t)}{dt} = \mathbf{F}(t)\mathbf{x}(t) + \mathbf{w}(t),$$

where

$$(2-3) \qquad \mathbf{F}(t) = \begin{bmatrix} 0 & 0 & 1 & 0 \\ 0 & 0 & 0 & 1 \\ 0 & 0 & 0 & 0 \\ 0 & 0 & 0 & 0 \end{bmatrix} \mathbf{x}(t) + \mathbf{w}(t),$$

$$(2-4) \qquad \mathbf{w}(t) = \begin{bmatrix} 0 & 0 & w_1(t) & w_2(t) \end{bmatrix}',$$

and $\mathbf{w}(t)$ is known as the process noise. We assume $w_i(t), i = 1,2$ as zero-mean white noise accelerations:

$$(2-5) \quad E\{w_i(t)\} = 0, \quad E\{w_i(t) w_j(t)'\} = q_i d_{ij} d(t-t),$$

where $q_i, i = 1,2$ are the power spectral densities of the process noise.

Let $\mathbf{x}_k := \mathbf{x}(t_k)$ denote the discrete time state of the target at time t_k. Discretization of (2-2) gives [5],[6]

$$(2-6) \quad \mathbf{x}_k = \Phi(k,k-1)\mathbf{x}_{k-1} + \mathbf{w}(k,k-1),$$

where $\Phi(k,k-1) := \Phi(t_k, t_{k-1})$ is the state transition matrix and $\mathbf{w}(k,k-1) := \mathbf{w}(t_k, t_{k-1})$ is the integrated process noise. The state transition matrix and the integrated process noise for the NCV motion are given by

$$(2-7) \quad \Phi(k,k-1) := \begin{bmatrix} 1 & 0 & \Delta_k & 0 \\ 0 & 1 & 0 & \Delta_k \\ 0 & 0 & 1 & 0 \\ 0 & 0 & 0 & 1 \end{bmatrix}, \quad \Delta_k = (t_k - t_{k-1}),$$

$$(2-8) \quad \mathbf{w}(k,k-1) = \int_{t_{k-1}}^{t_{kj}} \Phi(t_k, t) w(t) dt,$$

$$(2-9) \quad E\{\mathbf{w}(k,k-1)\} = 0,$$

$$(2-10) \quad E\{\mathbf{w}(j,j-1)\mathbf{w}'(k,k-1)\} = d_{jk}\mathbf{Q}(k,k-1).$$

$\mathbf{Q}(k,k-1)$ is the covariance of the process noise with the following form:

$$(2-11) \quad \mathbf{Q}(k,k-1) = \begin{bmatrix} \frac{1}{3}q_1(\Delta_k)^3 & 0 & \frac{1}{2}q_1(\Delta_k)^2 & 0 \\ 0 & \frac{1}{3}q_2(\Delta_k)^3 & 0 & \frac{1}{2}q_2(\Delta_k)^2 \\ \frac{1}{2}q_1(\Delta_k)^2 & 0 & q_1\Delta_k & 0 \\ 0 & \frac{1}{2}q_2(\Delta_k)^2 & 0 & q_2\Delta_k \end{bmatrix}.$$

3 GMTI Measurement Model

A GMTI radar sensor measures the range (r), azimuth (a), and range-rate $(\dot{r})$ of a target. The GMTI measurement model at time k is described by [3]

$$(3-1) \quad \mathbf{z}_k = \mathbf{h}(\mathbf{x}_k, \mathbf{s}_k) + \mathbf{v}_k,$$

where $\mathbf{s}_k \in \Re^3$ and $\mathbf{v}_k \in \Re^3$ are sensor position and measurement noise at time k, respectively:

$$(3-2) \quad \mathbf{s}_k := \begin{bmatrix} s_{kx} & s_{ky} & s_{kz} \end{bmatrix}',$$

$$(3-3) \quad \mathbf{v}_k := \begin{bmatrix} v_{kr} & v_{ka} & v_{k\dot{r}} \end{bmatrix}'.$$

We assume the sensor position $\mathbf{s}_k$ as error-free. We assume that $\mathbf{v}_k$ is a zero-mean independent Gaussian noise with diagonal covariance $\mathbf{R}_k$:

$$(3-4) \quad \mathbf{v}_k \sim N(0, \mathbf{R}_k),$$

$$(3-5) \quad \mathbf{R}_k = \begin{bmatrix} s_{kr}^2 & 0 & 0 \\ 0 & s_{ka}^2 & 0 \\ 0 & 0 & s_{k\dot{r}}^2 \end{bmatrix}.$$

Dropping the subscript k, the GMTI measurement model is described by

$$(3-6) \quad h_r(\mathbf{x},\mathbf{s}) = [(x-s_x)^2 + (y-s_y)^2 + s_z^2]^{1/2},$$

$$(3-7) \quad h_a(\mathbf{x},\mathbf{s}) = \begin{cases} \tan^{-1}(x-s_x, y-s_y), & \text{if } \tan^{-1}(x-s_x, y-s_y) > 0, \\ \tan^{-1}(x-s_x, y-s_y) + 2p, & \text{if } \tan^{-1}(x-s_x, y-s_y) < 0, \end{cases}$$

$$(3-8)\quad h_{\dot r}(\mathbf{x},\mathbf{s}) = \frac{(x-s_x)\dot x + (y-s_y)\dot y}{[(x-s_x)^2+(y-s_y)^2+s_z^2]^{1/2}}.$$

4 Iterated Extended Kalman Filter (IEKF)

Linearization is usually performed about the predicted state $\hat{\mathbf{x}}_{k|k-1}$ at time k. The measurement-updated state $\hat{\mathbf{x}}_{k|k}$ can be further improved by iteratively computing the updated state $\hat{\mathbf{x}}_{k|k}$, measurement gradient matrix $\mathbf{H}_k$, gain $\mathbf{K}_k$, and measurement updated covariance matrix $\mathbf{P}_{k|k}$. Let $\hat{\mathbf{x}}^i_{k|k}$, $\mathbf{H}_k(\hat{\mathbf{x}}^i_{k|k})$, $\mathbf{K}_k(\hat{\mathbf{x}}^i_{k|k})$, and $\mathbf{P}^i_{k|k}$ denote the values at the $i^{\text{th}}, i = 0,1,2,...$ iteration. A number of iterations are carried out until no significant change in the updated state is achieved. The steps of the iterated IEKF algorithm are given below:

State and covariance propagation

$$(4-1)\quad \hat{\mathbf{x}}_{k|k-1} = \Phi(k,k-1)\hat{\mathbf{x}}_{k-1|k-1},$$

$$(4-2)\quad \mathbf{P}_{k|k-1} = \Phi(k,k-1)\mathbf{P}_{k-1|k-1}\Phi'(k,k-1) + \mathbf{Q}(k,k-1),$$

State and covariance update

$$(4-3)\quad \hat{\mathbf{x}}^0_{k|k} = \hat{\mathbf{x}}_{k|k-1}, \qquad \text{initialization}$$

$$(4-4)\quad \hat{\mathbf{x}}^{i+1}_{k|k} = \hat{\mathbf{x}}_{k|k-1} + \mathbf{K}^i_k[\mathbf{z}_k - \mathbf{h}(\hat{\mathbf{x}}^i_{k|k}) - \mathbf{H}_k(\hat{\mathbf{x}}^i_{k|k})\{\hat{\mathbf{x}}_{k|k-1} - \hat{\mathbf{x}}^i_{k|k}\}],\ i = 0,1,...$$

$$(4-5)\quad \mathbf{K}^i_k = \mathbf{P}_{k|k-1}\mathbf{H}'_k(\hat{\mathbf{x}}^i_{k|k})\mathbf{G}^{-1}_k(\hat{\mathbf{x}}^i_{k|k}),\ i = 1,2,...$$

$$(4-6)\quad \mathbf{G}_k(\hat{\mathbf{x}}^i_{k|k}) = \mathbf{H}_k(\hat{\mathbf{x}}^i_{k|k})\mathbf{P}_{k-1|k-1}\mathbf{H}'_k(\hat{\mathbf{x}}^i_{k|k}) + \mathbf{R}_k,\quad i = 1,2,...$$

$$(4-7)\quad \mathbf{P}^{i+1}_{k|k} = [\mathbf{I} - \mathbf{K}_k(\hat{\mathbf{x}}^i_{k|k})\mathbf{H}_k(\hat{\mathbf{x}}^i_{k|k})]\mathbf{P}_{k|k-1},\quad i = 0,1,...$$

$$(4-8)\quad \mathbf{H}_k(\mathbf{x}^i_{k|k}) = \mathbf{H}(\mathbf{x}^i_{k|k},\mathbf{s}_k) := \left.\frac{\partial \mathbf{h}(\mathbf{x}_k,\mathbf{s}_k)}{\partial \mathbf{x}_k}\right|_{\mathbf{x}=\mathbf{x}^i_{k|k}}.$$

$\mathbf{G}_k(\hat{\mathbf{x}}^i_{k|k})$ represents the covariance of the innovations process.

Computation of measurement gradient matrix

Let $\mathbf{r}$ and $\mathbf{u}$ be the range vector and unit vector along the radar LOS, respectively:

$$(4-9)\quad \mathbf{r} := [x-s_x \quad y-s_y \quad -s_z]',$$

$$(4-10)\quad \mathbf{u} := \frac{\mathbf{r}}{h_r(\mathbf{x},\mathbf{s})} = \frac{1}{h_r(\mathbf{x},\mathbf{s})}[x-s_x \quad x-s_y \quad -s_z]'.$$

The measurement gradient matrix required in the measurement update step is

$$(4-11)\quad \mathbf{H}(\mathbf{x},\mathbf{s}) := \frac{\partial \mathbf{h}(\mathbf{x},\mathbf{s})}{\partial \mathbf{x}} = \begin{bmatrix} u_x & u_y & 0 & 0 \\ r_y/r^2 & -r_x/r^2 & 0 & 0 \\ (\dot x - \dot r u_x)/r & (\dot y - \dot r u_y)/r & u_x & u_y \end{bmatrix},$$

$$(4-12)\quad r^2 = (x-s_x)^2 + (y-s_y)^2.$$

Filter state initialization

Given the range and azimuth measurements (r_1, a_1) from the first GMTI measurement $\mathbf{z}_1$, the initial maximum likelihood estimate of the target position is

$$(4-13)\quad \begin{bmatrix}\hat x_1 \\ \hat y_1\end{bmatrix} = \begin{bmatrix} s_{1x} + \hat r_1 \sin a_1 \\ s_{1y} + \hat r_1 \cos a_1 \end{bmatrix},$$

$$(4-14)\quad \hat r_1 = [r_1^2 - s_{1z}^2]^{1/2}.$$

Assuming no error in the sensor position, the covariance of position error is

$$(4-15)\quad P_{1,xy}(1,1) = (\frac{r_1}{\hat r_1}\sin a_1)^2 s_r^2 + (\hat r_1 \cos a_1)^2 s_a^2,$$

$$(4-16)\quad P_{1,xy}(2,2) = (\frac{r_1}{\hat r_1}\cos a_1)^2 s_r^2 + (\hat r_1 \sin a_1)^2 s_a^2,$$

$$(4-17)\quad P_{1,xy}(1,2) = P_{1,xy}(2,1) = \frac{\sin 2a_1}{2}[(\frac{r_1}{\hat r_1})^2 s_r^2 - \hat r_1^2 s_a^2].$$

The velocity of the target can not be observed from a single measurement of range-rate. For simplicity, we set the initial velocity to zero and standard deviations of the X and Y components of the velocity to the maximum feasible velocity $v_{\max}$. Thus the initial state estimate and covariance using the first range and azimuth measurement are

$$(4-18)\quad \hat{\mathbf{x}}_0 = [\hat x_1 \quad \hat y_1 \quad 0 \quad 0]',$$

$$(4-19)\quad \mathbf{P}_0 = \begin{bmatrix} \mathbf{P}_{1,xy} & 0_{2\times1} & 0_{2\times1} \\ 0_{1\times2} & v^2_{\max} & 0_{1\times2} \\ 0_{1\times1} & 0_{1\times1} & v^2_{\max} \end{bmatrix}.$$

Then the first range-rate measurement $\dot r_1$ is used to update the state and covariance in (4-18) and (4-19)

5 Recursive Bayesian Estimation

A general discrete time dynamics for the state $\mathbf{x}_k \in \Re^n$ of a system is described by [8]

$$(5-1) \quad \mathbf{x}_k = \mathbf{f}_{k-1}(\mathbf{x}_{k-1}, \mathbf{w}_{k-1}),$$

where $\mathbf{f}_{k-1} : \Re^n \times \Re^p \to \Re^n$ is the system evolution function and $\mathbf{w}_{k-1} \in \Re^p$ is a white noise sequence (known as the process noise) independent of the past and current states. We assume that the probability density (pdf) of $\mathbf{w}_{k-1}$ is known. The function $\mathbf{f}_{k-1}$ may be a linear or nonlinear function of $\mathbf{x}_{k-1}$ and $\mathbf{w}_{k-1}$, and the pdf of $\mathbf{w}_{k-1}$ may be arbitrary.

We assume that measurements $\{\mathbf{z}_k \in \Re^m\}$ are available at discrete times and a functional relationship between the measurement $\mathbf{z}_k$ and the state $\mathbf{x}_k$ is known:

$$(5-2) \quad \mathbf{z}_k = \mathbf{h}_k(\mathbf{x}_k, \mathbf{v}_k),$$

where $\mathbf{h}_k : \Re^n \times \Re^r \to \Re^n$ is the measurement model function and $\mathbf{v}_k \in \Re^r$ is a white noise sequence (known as the measurement noise) with known pdf. We assume that $\mathbf{v}_k$ is independent of the past and current states and process noise. The measurement function $\mathbf{h}_k$ may be a linear or nonlinear function of $\mathbf{x}_k$ and $\mathbf{v}_k$, and the pdf of $\mathbf{v}_k$ may be arbitrary. Let $\mathbf{Z}_k$ denote the set of measurements $\{\mathbf{z}_1, \mathbf{z}_2, ..., \mathbf{z}_k\}$.

Our objective is to compute the conditional density $p(\mathbf{x}_k \mid \mathbf{Z}_k)$ of the state $\mathbf{x}_k$ given all the measurements $\mathbf{Z}_k$ at time k. Suppose $p(\mathbf{x}_{k-1} \mid \mathbf{Z}_{k-1})$ is known. Then $p(\mathbf{x}_k \mid \mathbf{Z}_k)$ can be computed from $p(\mathbf{x}_{k-1} \mid \mathbf{Z}_{k-1})$ using the prediction and the measurement update steps. Using the prediction step, the prior pdf of the state at time t_k is given by

$$(5-3) \quad p(\mathbf{x}_k \mid \mathbf{Z}_{k-1}) = \int p(\mathbf{x}_k \mid \mathbf{x}_{k-1}) p(\mathbf{x}_{k-1} \mid \mathbf{Z}_{k-1}) d\mathbf{x}_{k-1},$$

where $p(\mathbf{x}_k \mid \mathbf{x}_{k-1})$ is known as the state transition density and is determined by the system dynamics model (5-1). Then prior pdf of the state $p(\mathbf{x}_k \mid \mathbf{Z}_{k-1})$ can be updated at time k by Bayes' rule using the measurement $\mathbf{z}_k$:

$$(5-4) \quad p(\mathbf{x}_k \mid \mathbf{Z}_k) = \frac{p(\mathbf{z}_k \mid \mathbf{x}_k) p(\mathbf{x}_k \mid \mathbf{Z}_{k-1})}{p(\mathbf{z}_k \mid \mathbf{Z}_{k-1})},$$

where

$$(5-5) \quad p(\mathbf{z}_k \mid \mathbf{Z}_{k-1}) = \int p(\mathbf{z}_k \mid \mathbf{x}_k) p(\mathbf{x}_k \mid \mathbf{Z}_{k-1}) d\mathbf{x}_k .$$

$p(\mathbf{z}_k \mid \mathbf{x}_k)$ is known as the likelihood function and is determined by the measurement model (5-2).

Equations (5-4) and (5-5) represent a general recursive solution for the state estimation problem in the Bayesian framework. These equations are valid for any pdf of the state, process noise, and measurement noise with general system dynamics and measurement models. However, closed form solutions are not always possible. When $\mathbf{f}_k$ and $\mathbf{h}_k$ are linear, and $\mathbf{w}_k$ and $\mathbf{v}_k$ are additive Gaussian noises with known pdf, (5-4) and (5-5) give rise to the well-known Kalman filter (KF) algorithm. Since $\mathbf{h}_k$ for the GMTI measurement model is nonlinear, the EKF is not an optimal estimator for the problem.

Given $\mathbf{Z}_k$, the conditional mean estimator [4],[6]

$$(5-6) \quad \hat{\mathbf{x}}_{k|k} := E\{\mathbf{x}_k \mid \mathbf{Z}_k\} = \int \mathbf{x}_k \, p(\mathbf{x}_k \mid \mathbf{Z}_k) d\mathbf{x}_k$$

represents the minimum variance or minimum mean-square error (MMSE) estimator. The covariance of the conditional mean estimate is given by [4],[6]

$$(5-7) \quad \mathbf{P}_{k|k} := E\{(\mathbf{x}_k - \hat{\mathbf{x}}_{k|k})(\mathbf{x}_k - \hat{\mathbf{x}}_{k|k})' \mid \mathbf{Z}_k\} = \int (\mathbf{x}_k - \hat{\mathbf{x}}_{k|k})(\mathbf{x}_k - \hat{\mathbf{x}}_{k|k})' p(\mathbf{x}_k \mid \mathbf{Z}_k) d\mathbf{x}_k .$$

6 Particle Filter (PF)

Particle filters approximate the continuous conditional pdf $p(\mathbf{x}_k \mid \mathbf{Z}_k)$ by an independent set of random samples (also known as particles) $\{\mathbf{x}_k^i\}_{i=1}^N$ and associated positive weights $\{w_k^i > 0\}_{i=1}^N$ [8],[12],[14]. The PF is an algorithm for propagating and updating the samples and weights numerically such that the random samples are approximately distributed as independent samples arising from the pdf $p(\mathbf{x}_k \mid \mathbf{Z}_k)$. The numerical approximation for the prediction step is

$$(6-1) \quad p(\mathbf{x}_k \mid \mathbf{Z}_{k-1}) = \int p(\mathbf{x}_k \mid \mathbf{x}_{k-1}) p(\mathbf{x}_{k-1} \mid \mathbf{Z}_{k-1}) d\mathbf{x}_{k-1} \approx (1/N) \sum_{i=1}^{N} p(\mathbf{x}_k \mid \mathbf{x}_{k-1} = \mathbf{x}_{k-1}^i),$$

where $\{\mathbf{x}_{k-1}^i\}_{i=1}^N$ are N independent, identically distributed (iid) samples drawn from $p(\mathbf{x}_{k-1} \mid \mathbf{Z}_{k-1})$.

The detailed steps of the PF with sampling importance resampling (SIR) [8],[12],[14],[15] are:

1. Select the number of particles (N) to be generated and the threshold for resampling (N_{thres}) [9],[15]
2. Initialization
   Set $k = 1$.
   Generate N samples $\{\mathbf{x}_1^i\}_{i=1}^N$ from the prior density $p_0(\mathbf{x}_1)$.
   Set $\{w_1^i = 1/N\}_{i=1}^N$.

3. Increment k: $k{=}k{+}1$
4. Prediction

Generate N samples $\{\mathbf{w}^i(k,k-1) \sim N(0,\mathbf{Q}(k,k-1)\}_{i=1}^N$.

Compute N predicted state vectors:
$\{\mathbf{x}_k^i = \Phi(k,k-1)\mathbf{x}_{k-1}^i + \mathbf{w}^i(k,k-1)\}_{i=1}^N$.

5. State update with measurement $\mathbf{z}_k$

Compute the likelihoods: $\{p(\mathbf{z}_k \mid \mathbf{x}_k^i)\}_{i=1}^N$.

Update the weights: $\{w_k^i = \dfrac{w_{k-1}^i p(\mathbf{z}_k \mid \mathbf{x}_k^i)}{\sum_{i=1}^N w_{k-1}^i p(\mathbf{z}_k \mid \mathbf{x}_k^i)}\}_{i=1}^N$

Compute the measurement updated state estimate:

$$\hat{\mathbf{x}}_{k|k} = \sum_{i=1}^N w_k^i \mathbf{x}_k^i$$

6. Compute effective sample size (N_{eff})

$$N_{\text{eff}} = 1/\sum_{i=1}^N (w_k^i)^2.$$

If $N_{\text{eff}} > N_{\text{thres}}$, then

- Go to step 3.

Else

- Resample a new set $\{\mathbf{x}_k^{i^*}\}_{i=1}^N$ by sampling with replacement N times from the discrete set $\{\mathbf{x}_k^i\}_{i=1}^N$ where $\Pr(\mathbf{x}_k^{i^*} = \mathbf{x}_k^j) = w_k^j$.
- Set $\{w_k^i = 1/N\}_{i=1}^N$.
- Go to step 3.

End

7 Simulation and Results

The geometry of the nominal target trajectory and sensor trajectory is shown in Figure 1. The standard deviations of the range, azimuth, and range-rate for the sensor measurements are 20 meters, 0.001 radian, and 1 m/s, respectively. The height and speed of the sensor are 10,000 m above the XY plane and 166.7 m/s, respectively. Each component of the power spectral density (q_1, q_2) of the process noise used for simulating the truth trajectory is 0.1 m^2s^{-3}. We used The same values of the power spectral density (q_1, q_2) of the process noise in the IEKF and PF. Results presented in Figures 2-8 are based on sensor measurements with a revisit time of two seconds. The truth trajectory of the target and GMTI report locations from range and azimuth are shown in Figure 2. The truth trajectory, IEKF, and PF estimated trajectories, and IEKF and PF estimated velocities are shown in Figures 3-8 on page 7 at the end of the paper for easy comparison of the IEKF and PF solutions. We used 20,000 random samples in the PF algorithm. The root mean square (RMS) position and velocity estimation errors using the IEKF and PF are presented in Table 1.

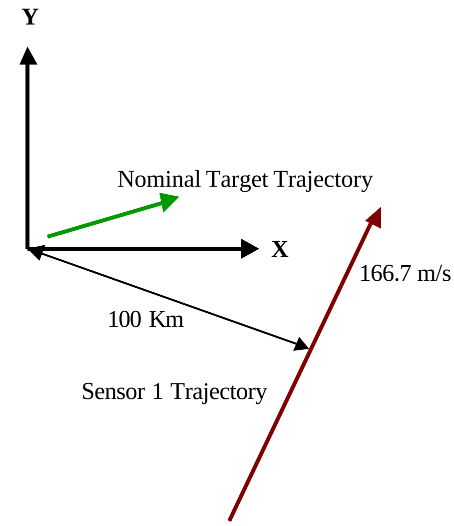

Figure 1. Nominal Target and Sensor Geometry

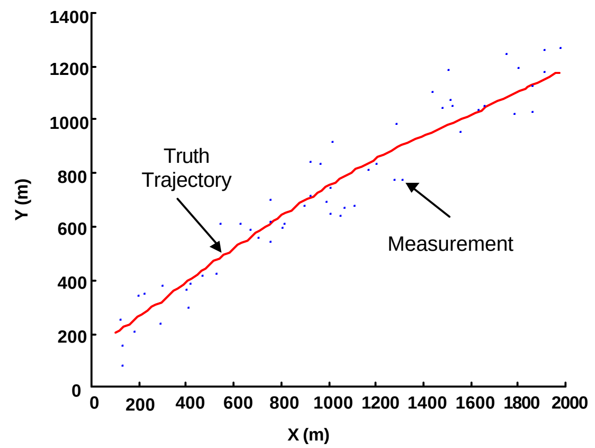

Figure 2. Truth Trajectory and GMTI Report Locations

Table 1. Comparison of position and velocity estimation errors of the IEKF and PF

Algorithm	RMS Position Error (m)	RMS Velocity Error (m/s)
IEKF	65.935	3.243
PF	64.598	2.664

8 Conclusions

We have performed a preliminary comparative study of the IEKF and PF algorithms applied to the GMTI tracking problem. The numerical results show that the accuracies of the position estimation of the two algorithms are comparable. The velocity estimation accuracy of the PF is higher than that of the IEKF. We plan to use more efficient PF algorithms in our future work. We also plan to analyze the performance of the IEKF, IMM, and PF algorithms using realistic GMTI tracking scenarios which includes motion of the target on the three dimensional terrain and road-network using the degree of nonlinearity of the GMTI measurement model as an independent variable. The degree of nonlinearity is based on concepts of differential geometry and uses the parameter-effects curvature and intrinsic curvature of the measurement model.

References

[1] J. N. Entzminger, Jr., C. A. Fowler, and W. J. Kenneally, JointSTARS and GMTI, Past, Present, and Future, *IEEE Transactions on Aerospace and Electronic Systems*, vol. 35, pp. 748-761, April 1999.
[2] A. H. Jazwinski, *Stochastic Processes and Filtering Theory*, Academic Press, 1970.
[3] J. R. Moore and W. D. Blair, Practical Aspects of Multisensor Tracking, in *Multitarget-Multisensor Tracking: Applications and Advances*, Volume III ,Y. Bar-Shalom and William Dale Blair, (ed.) pp. 1-76, Artech House, 2000.
[4] B. D. O. Anderson and J. B. Moore, *Optimal Filtering*, Prentice Hall, 1979.
[5] A. Gelb, Ed., *Applied Optimal Estimation*, The MIT Press, 1974.
[6] Y. Bar-Shalom and X. R. Li, *Estimation and Tracking: Principles, Techniques, and Software*, Artech House, 1993 (reprinted by YBS Publishing, 1998).
[7] H. A. P. Blom, and Y. Bar-Shalom, The Interacting Multiple Model Algorithm for Systems with Markovian Switching Coefficients, IEEE Transactions on Automatic Control, 22(3): 302-312, 1977
[8] N. J. Gordon, D. J. Salmond, and A. F. M. Smith, Novel approach to nonlinear/nonGaussian Bayesian state estimation, *IEE Proceedings-F*, vol. 140, pp. 107-113, April 1993.
[9] A. Doucet, On sequential Monte Carlo sampling methods for Bayesian filtering, Technical Report, University of Cambridge, 1998.
[10] J. S. Liu and R. Chen, Sequential Monte Carlo methods for dynamic systems, *Journal of the American Statistical Assoc.*, vol. 93, pp. 1032-1044, 1998.
[11] J. Carpenter, P. Clifford, and P. Fernhead, An improved particle filter for nonlinear problems, *IEE Proceedings-Radar, Sonar, Navig.* , vol. 146, pp. 2-7, Feb. 1999.
[12] N. Bergman, *Recursive Bayesian Estimation, Navigation and Tracking Applications*, Ph.D. thesis, Linkoping University, Sweden, 1999.
[13] P. Fernhead, *Sequential Monte Carlo methods in filter theory*, Ph.D. thesis, Merton College, University of Oxford,1998.
[14] S. Challa and N. Gordon, Target Tracking Using Particle Filters, Proceedings of the Workshop on Estimation, Tracking, and Fusion: A Tribute to Yaakov Bar-Shalom, Monterey, CA, May 2001.
[15] Sanjeev Arulampalam and Branko Ristic, Comparison of the Particle Filter with Range-Parametrised and Modified Polar EKFs for Angle-Only Tracking, Signal and Data Processing of Small Targets 2000, Oliver E. Drummond, Ed., Proceedings of the SPIE, vol. 4048, pp. 288-299, 2000.

Iterated Extended Kalman Filter (IEKF) and Particle Filter (PF) Estimates

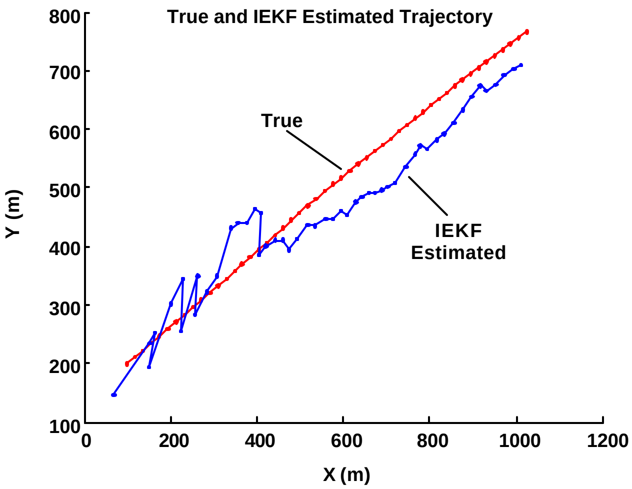

Figure 3. Truth and IEKF Estimated Trajectories

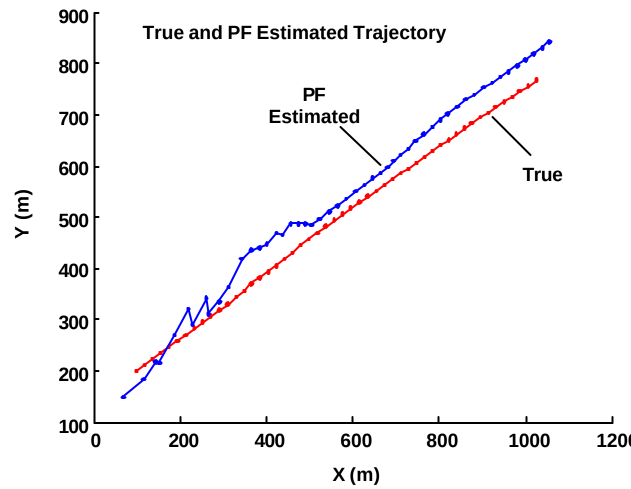

Figure 4. Truth and PF Estimated Trajectories

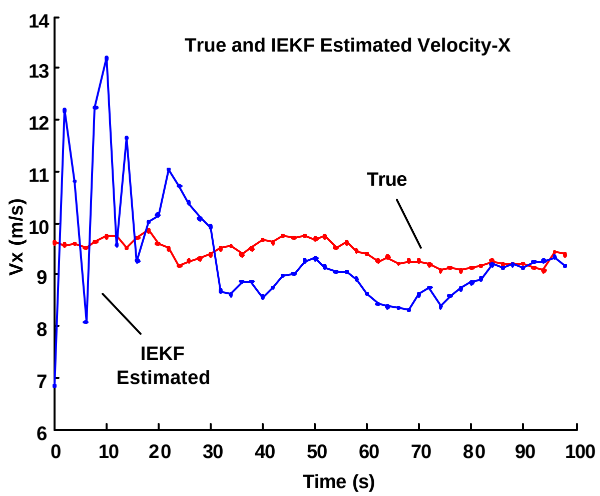

Figure 5. Truth and IEKF Estimated Velocity-X

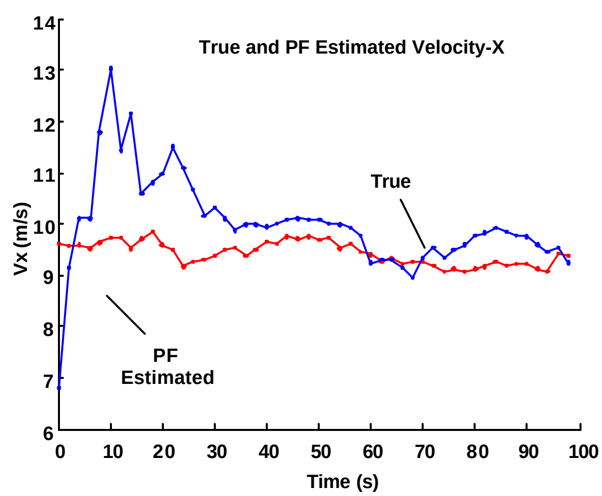

Figure 6. Truth and PF Estimated Velocity-X

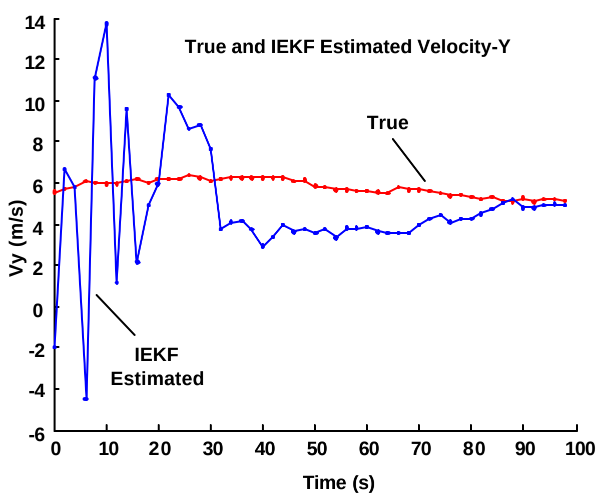

Figure 7. Truth and IEKF Estimated Velocity-Y

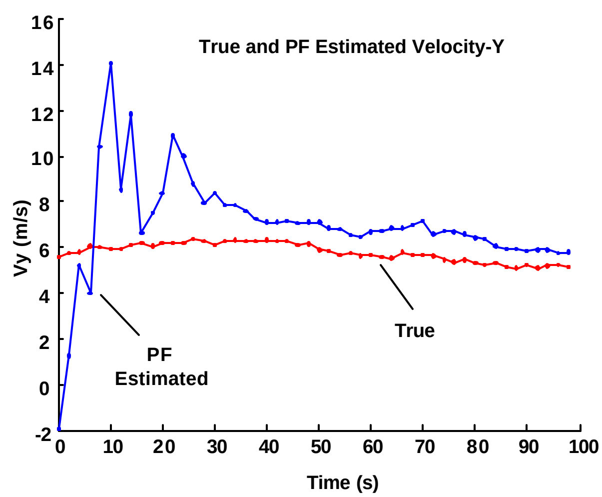

Figure 8. Truth and PF Estimated Velocity-Y